The Journal of Veterinary Medical Science

NOTE

Wildlife Science

Clinical and pathological characteristics of acute myelogenous leukemia in a female koala with diabetes mellitus

Nanao ITO[1)], Toshinori YOSHIDA[2)]*, Rho ICHIKAWA[2)], Emi MAKINO[3)], Satoshi AKEMA[3)], Junko FUKUMORI[3)], Naofumi TAKAHASHI[3)], Junta NAKAHARA[2)], Risako YAMASHITA[2)], Kai ORIHARA[2)], Mio KOBAYASHI[2)], Hou XIANTAO[2,4)], Yousuke WATANABE[2)], Sayaka MIZUKAMI[2)] and Makoto SHIBUTANI[2)]

[1)]Hirakawa Zoological Park, 5669-1 Hirakawa-cho, Kagoshima-shi, Kagoshima 891-0133, Japan
[2)]Laboratory of Veterinary Pathology, Tokyo University of Agriculture and Technology, 3-5-8 Saiwai-cho, Fuchu-shi, Tokyo 183-8509, Japan
[3)]The Institute of Environmental Toxicology, 4321 Uchimoriya-machi, Joso-shi, Ibaraki 303-0043, Japan
[4)]Department of Pet Science and Technology, Shandong Vocational Animal Science and Veterinary College, Weifang 261061, Shandong Province, China

J. Vet. Med. Sci.
81(8): 1229–1233, 2019
doi: 10.1292/jvms.19-0006

Received: 6 January 2019
Accepted: 11 June 2019
Advanced Epub: 2 July 2019

ABSTRACT. A female koala presented with hyperglycemia related to diabetes mellitus diagnosed at 9 years and treated with insulin. She presented with nasal hemorrhage, anemia, leukocytosis, and tachypnea at 10 years. A blood smear examination revealed scattered, atypical large myeloid cells and a clinical diagnosis of myelogenous leukemia was made. White blood cell count reached a maximum of $295 \times 10^2/\mu l$, with evidence of severe regenerative anemia and thrombocytopenia. Grossly, systemic lymph node enlargement, fragile liver with hemorrhage, and bloody ascites were observed. Histopathologically, atypical myeloid cells, including myelocytic and metamyelocytic cells, were scattered in the vasculature and surrounding tissues throughout the organs. The patient was infected with a koala retrovirus, which might have caused the myelogenous leukemia.

KEY WORDS: anemia, diabetes, koala, myelogenic leukemia, retrovirus

The koala retrovirus (KoRV) is a gammaretrovirus which shares 78% nucleotide identity with the gibbon ape leukemia virus [4, 9] and induces lymphoma and leukemia, and immune deficiencies associated with opportunistic infections in Australia [4, 11] and other countries such as Germany [3], U.S.A. [13], and Japan [8]. Lymphoma is demonstrated by single or multiple solid tumors affecting all lymphoid tissues or specific lymph nodes [5] and is subdivided into T-cell [1] and B-cell lymphoma [7]. An analysis of 51 samples from New South Wales and Queensland showed that T-cell lymphoma is relatively predominant when compared with B-cell lymphoma [2]. Beside lymphoid leukemia [2], non-lymphoid leukemia was not examined in detail. Myeloid lineage leukemia has been reported, although definitive identification of cell lineage has not been attempted in most cases [5, 12]. We encountered the case of a koala with a possible acute myelogenous leukemia, and herein report its clinical and pathological characteristics.

A 9-year and 5-month-old female koala, which had been raised at a zoo in Japan, showed hyperglycemia in a routine clinical examination, and was diagnosed with diabetes mellitus. She was treated with insulin (Tresiba, mean 1.0 U/day, SC, Novo nordisk Co., Ltd., Tokyo, Japan) to control plasma glucose levels. No diabetes-related clinical signs were observed thereafter. At 10-year and 4-months of age, she showed bilateral nasal hemorrhage, with no evidence of facial trauma. No bacterial and fungal colonies were cultured from nasal swab samples. On day 2, a hematological examination revealed that mild decreases in red blood cell count (RBC, 282×10^4/m*l*), hemoglobin (HGB, 9.8 g/d*l*), and hematocrit (HCT, 32.8%) (Fig. 1A and 1B). She showed slight decreased food intake. On day 7, nasal hemorrhage was confirmed. On day 9, an X-ray revealed no abnormalities in the thoracic and abdominal cavities. Hematological examination revealed anemia, i.e. lower RBC (228×10^4/m*l*), HGB (7.9 g/d*l*), and HCT (26.9%) with a normal of white blood cell count (WBC, $36 \times 10^2/\mu l$). On blood smears, erythroblasts were observed, together with atypical large myeloid cells (Fig. 1C and 1D). No blood coagulation abnormalities were detected. She was administered anti-hemorrhagic drugs, i.e. carbazochrome sodium sulfonate (Auzei 10 mg, approximately 2 mg/kg, IM, SID, Nichi-Iko Pharmaceutical Co., Ltd., Toyama, Japan) and tranexamic acid (Transamin, approximately 10 mg/kg, IM, SID, Daiichi

*Correspondence to: Yoshida, T.: yoshida7@cc.tuat.ac.jp

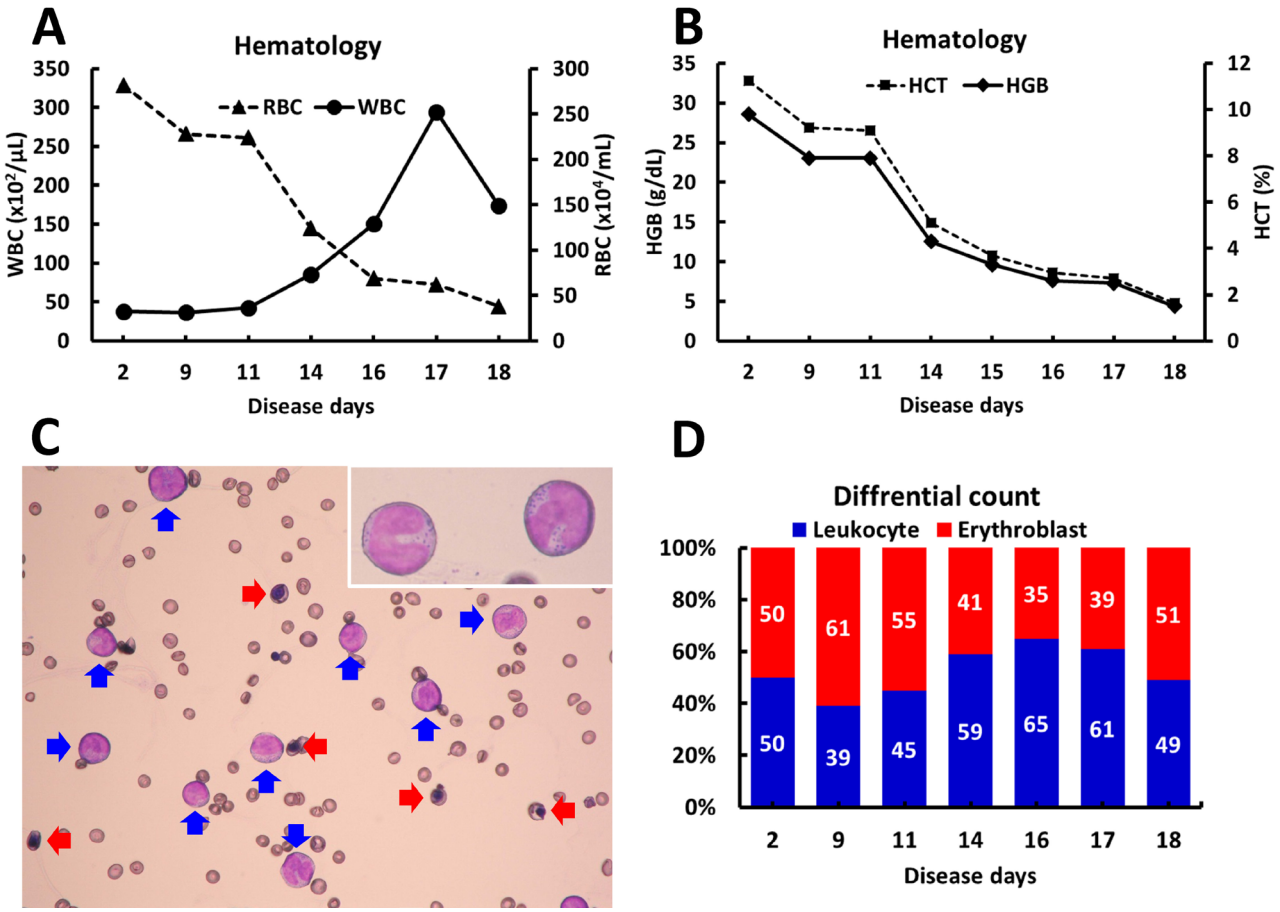

Fig. 1. Hematology. (A, B) A time-course observation of white blood cell count (WBC), red blood cell count (RBC) (A), hematocrit (HCT) and hemoglobin (HGB) (B) during the period of the disease. WBC is shown as "corrected WBC" as described in the texts. (C) Atypical myeloid cells (blue arrows) and erythroblasts (red arrows) are observed on blood smears. Inset: Atypical myeloid cells contain azurophilic granules in the cytoplasm. Magnification: ×400; inset ×1,000. (D) Differential cell count on blood smears to separate leukocytes and erythroblasts at each time point.

Sankyo Co., Ltd., Tokyo, Japan). She was also administered an antibiotics Orbifloxacin (Victas S, 5 mg/kg, SC, SID, DS Pharma Animal Health Co., Ltd., Osaka, Japan) and antifungal drug Itraconazole (Itrizole Oral Solution 1%, 50 mg/kg, PO, SID, Janssen Pharmaceutical K. K., Tokyo, Japan) to prevent opportunistic infections. On day 11, she was administered water-soluble vitamins (Lesthionin C, 0.7 m*l*/head, SC, SID, Kyorittsuseiyaku Co., Tokyo, Japan) to preserve malnourishment. On day 11, hematology revealed a slight increase in WBC (42 × $10^2/\mu l$), and decreased RBC (224 × 10^4/m*l*), HGB (7.9 g/d*l*) and HCT (26.5%). On day 13, enlargement of bilateral submandibular lymph nodes was detected on palpation. On day 14, a diagnosis of leukemia was made, based on the hematological findings, a 2-fold increase in WBC (86 × $10^2/\mu l$) as compared with that on day 2, with evidence of anemia: decreased RBC (124 × 10^4/m*l*), HGB (4.3 g/d*l*) and HCT (14.9%). She was administered fat-soluble vitamins (Vitalera; 0.01 m*l*/head, SC, SID; Fujita Pharmaceutical Co., Ltd., Tokyo Japan) and eucalyptus peisuto by forced feeding. On day 15, she was administered high-dose vitamin C (VC500, 300 mg/kg, IV, Nichi-Iko Pharmaceutical Co., Ltd.), L-Sodium lactate Ringer solution (Solulact, 10–16 m*l*/kg, IV and SC, Terumo Corporation, Tokyo, Japan), prednisolone (Prednisolone KS, 5 mg/kg, SC, SID, Kyoritsuseiyaku Co.), hepatotonic drug glutathione (Glutathione 200 mg Taiyo, 50 mg/head, IV and SC, SID, Teva Takeda Pharma Ltd., Nagoya, Japan), methyl methionine sulfonium chloride (Thiospen 400 mg, 100 mg/head, IV and SC, SID, Taiyo Yakuhin Osaka Hanbai Co., Ltd., Osaka, Japan), H2 blocker cimetidine (Tagamet 200 mg, 10 mg/kg, SC, SID, Sumitomo Dainippon Pharma Co., Ltd., Osaka, Japan). On day 16, however, she showed debility and severely decreased food intake, defecation, and urination. Her WBC continued to increase (150 × $10^2/\mu l$), with worsening of anemia and decreases in RBC (69 × 10^4/m*l*), HGB (2.6 g/d*l*), and HCT (8.6%). On day 17, she was placed in an oxygen box, because she showed severely decreased appetite, hypochondriasis, decreased motor activity, arrhythmia, and tachypnea. Her leukocytosis reached a peak at 295 × $10^2/\mu l$, with further worsening of anemia (RBC 62 × 10^4/m*l*, HGB 2.5 g/d*l*, and HCT 7.9%). On day 18, enlarged submandibular lymph nodes were re-confirmed by palpation. Hematology revealed an increase in WBC (173 × $10^2/\mu l$), severe anemia (RBC 38 × 10^4/m*l*, HGB 1.5 g/d*l*, and HCT 4.8%), and thrombocytopenia (platelet count, 0.1 × $10^4/\mu l$), hypokalemia (K, 2.1 mEq/*l*) and a raised aspartate transaminase (265 U/*l*). On day 19, she evidenced decreased body temperature and convulsions and then died. Leukocytes including atypical large myeloid cells and erythroblasts were detected on blood smears (Fig. 1C). Since erythroblasts might

apparently increase "automated WBC", "corrected WBC" was shown by calculating percentage of leukocytes and erythroblasts per 100 cells on the smears at each time point (Fig. 1A and 1D).

Grossly, generalized lymph node enlargement, masses in the liver with hemorrhage, and bloody ascites (approximately 2 m*l*) were observed. Variable-sized acinous masses (approximately ≤1 cm in diameter) were evident in the cervical and axillary lymph nodes. The fragile liver contained multiple masses (approximately ≤5 cm in diameter) and blood clots on the surface. Besides, red spots (approximately ≤5 mm in diameter) were observed covering the outside of the pericardium. Intraluminal contents (feed) were found in the stomach and intestines. Tissues were cut up into small pieces and fixed in 10% neutral-buffered formalin and embedded in paraffin. After embedding, 3-μm sections were prepared and stained with hematoxylin and eosin (HE) and Giemsa. Additional sections were subjected to immunohistochemistry (IHC) for myeloperoxidase (rabbit polyclonal, 1:100, Abcam Inc., Tokyo, Japan) and insulin (guinea pig, 1:200, DAKO, Glostrup, Denmark) with antigen retrieval by microwaving at 90°C for 10 min in 10 mM citrate buffer (pH 6.0). Expression was detected using a VECTASTAIN® Elite ABC kit (Vector Laboratories, Inc., Burlingame, CA, U.S.A.) with 3,3′-diaminobenzidine/hydrogen peroxide as the chromogen. The sections were then counterstained with hematoxylin.

Histopathologically, atypical myeloid cells were scattered in the vasculature and the surrounding tissues throughout the organs (Fig. 2A and 2B). The variable-sized myeloid cells had oval, band- or donut-shaped, or segmented nuclei and weakly eosinophilic cytoplasm containing azurophilic granules, which might be myelocytes, metamyelocytes, or immature neutrophils (stab-form), respectively. Frequently mitosis was observed in these cells. Foci of atypical myeloid cells with irregular shaped nuclei were

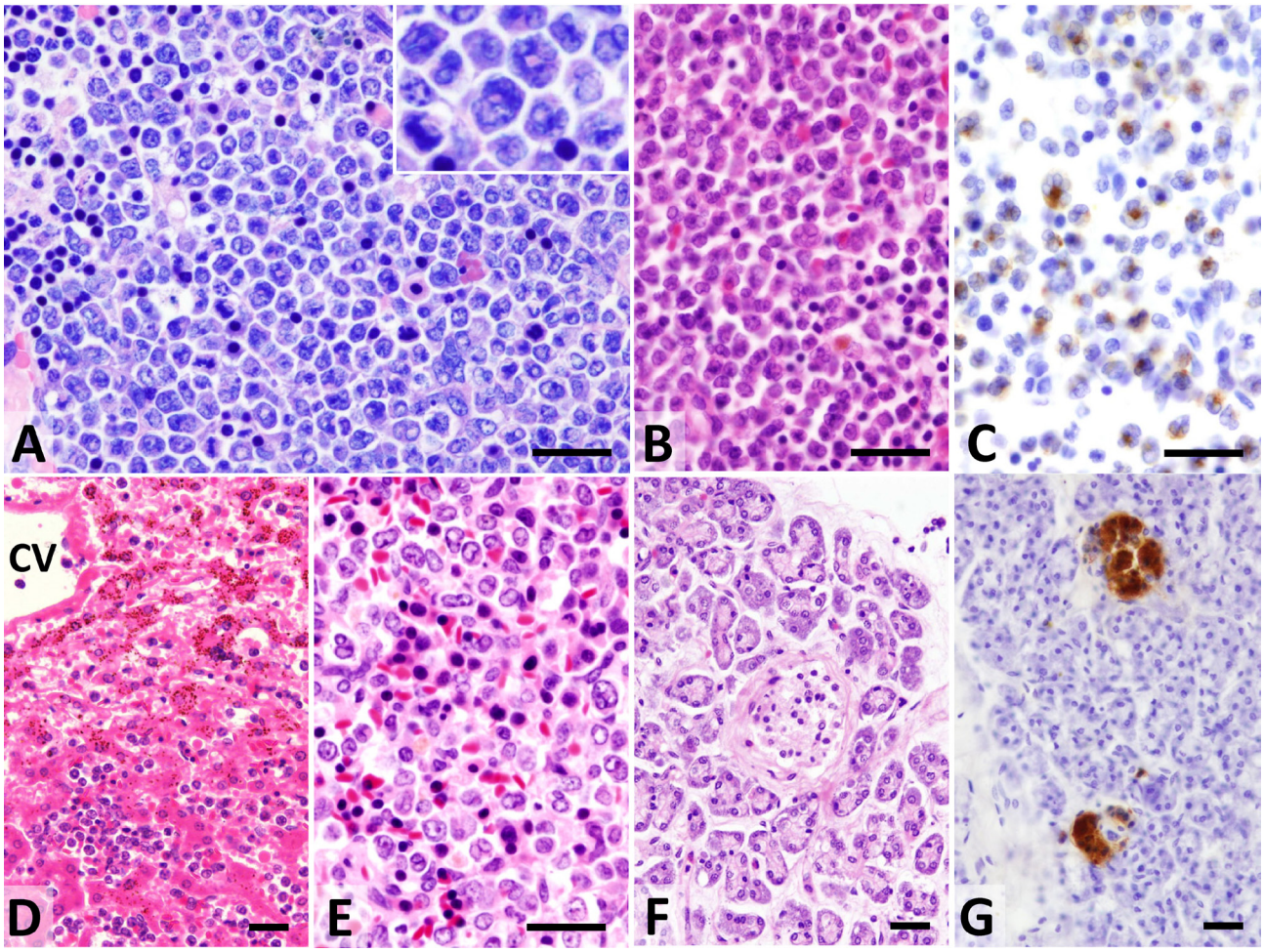

Fig. 2. Histopathological findings. (A) Variable-sized, atypical myeloid cells accumulate in the paracortex of the axillary lymph node. Erythroblasts (nucleated erythrocytes) are scattered. Inset: a higher magnification of atypical myeloid cells. Giemsa stain. (B) Atypical myeloid cells, erythroblasts (nucleated erythrocytes), and brown-pigment (hemosiderin)-contained macrophage are observed in the paracortex of the axillary lymph node. HE stain. (C) Several atypical myeloid cells express myeloperoxidase in the cytoplasm. IHC for myeloperoxidase. (D) Atypical myeloid cells and erythroblasts (nucleated erythrocytes) accumulate in a dilated sinusoid in the liver. Centrilobular hepatocytes are atrophic and containe small brown granules (lipofuscin) in the cytoplasm. CV: central vein. HE stain. (E) Extramedullary hematopoiesis, i.e., increases in erythroblasts is evident in the spleen. HE stain. (F) Langerhans island is atrophic with surrounding interstitial fibrosis in the pancreas. HE stain. (G) Atrophic Langerhans island expresses insulin in the cytoplasm. IHC for insulin. (A–G) Bar=50 μm.

sometimes noted, and a population of the atypical myeloid cells expressed myeloperoxidase (Fig. 2C). Erythroblasts were mixed with atypical myeloid cells. In the lymph nodes, atypical myeloid cells filled the sinusoids, together with erythroblasts and histiocytes phagocytosing erythrocytes. Lymph follicles and paracortex were extremely atrophic and often replaced by a diffuse proliferation of atypical myeloid cells, which were also observed in the sinus. In the heart, atypical myeloid cells had infiltrated the pericardium and surrounding cardiac tissues. In the lungs, atypical myeloid cells were observed in the interstitial and alveolar vasculature and sometimes in intra-alveolar spaces. In the liver, atypical myeloid cells were diffusely distributed in sinusoids leading to hepatic cord atrophy and the hepatocytes contained brown intracytoplasmic pigments (lipofuscin) (Fig. 2D). Cystic dilatation of sinusoids filled with atypical myeloid cells was also frequently observed throughout liver tissue, resembling peliosis hepatis. Centrilobular or focal hepatocellular necrosis was often observed. Periportal and sinusoidal fibrosis was observed in some regions of the liver tissue, containing foci of atypical myeloid cells. In the kidney, atypical myeloid cells were restricted to the interstitial vasculature and occasionally trapped in glomeruli. Mild interstitial fibrosis was observed in the cortex and medulla. In the spleen, atypical myeloid cells, together with apoptotic cells, were mainly distributed in the red pulp, while the white pulp was severely atrophic. Extramedullary hematopoiesis with prominent erythroblasts was evident in the red pulp (Fig. 2E). Mild perivascular fibrosis with brown pigment (hemosiderin) deposition was noted in some areas. In the adrenal gland, atypical myeloid cells were restricted to the vasculature in the medulla. In the submandibular gland, focal hyperplasia of ductal cells was found. In the stomach and intestines, a small number of atypical myeloid cells was scattered in the lamina propria. In the pancreas, Langerhans islands (expressed insulin) were severely atrophic, and mild, diffuse interstitial fibrosis was observed (Fig. 2F and 2G). The ovary was atrophic, and contained follicular cysts, hematoma, and atretic follicles. In the uterus, an endometrial stromal polyp and endometrial hyperplasia were observed, and atypical myeloid cells were found in the vasculature in the polyp. The nasal cavity contained small hamartoma nodules containing nasal glands and arteries.

The present case was characterized by acute onset of clinical symptoms with time-dependent leukocytosis with severe anemia and thrombocytopenia. A significant increase in atypical myeloid cells in blood smears was confirmed and a diagnosis of myelogenous leukemia was made. As the koala was infected with KoRV as reported previously [11], the case might be suspected to be a KoRV-related leukemia [5]. Histopathologically, lymph nodes, including enlarged submandibular lymph nodes, demonstrated severe infiltration of atypical myeloid cells with differentiation from myelocytes to immature neutrophils. Koalas often developed lymphoma and leukemia; however, no effective therapeutic treatment has been reported. Our symptomatic treatment could not improve the disease condition, but possibly prevented secondary, opportunistic infections, such as with bacteria, fungi, and chlamydia, which were often observed in koalas with lymphoma and leukemia [5].

The present koala showed hepatic dysfunction and diabetes. The hepatic dysfunction was probably caused by prominent hepatocellular necrosis and fibrosis, possibly related to intrahepatic infiltration with leukemic cells. She was also diagnosed with diabetes which was confirmed by the pathological findings in the pancreas, i.e., atrophy of Langerhans islands and interstitial fibrosis. Several cases of diabetes have been reported in koalas. In a case of koala with diabetes, the clinical examination revealed hyperglycemia, hypoproteinemia, glycosuria, and ketonuria and the pathological examination in the pancreas exhibited vacuolation and necrosis of Langerhans cells [10]. Diffuse interstitial fibrosis in the pancreas in the current case was similar to that of koala in the previous case report [6]. The mechanism for pancreatic atrophy and fibrosis is unknown; however, secondary inflammation in the pancreatic ducts and bile ducts from the gastrointestinal tract might cause the pancreatic and hepatic lesions [6]. Other miscellaneous changes noted in the ovary and uterus might cause infertility.

In koalas, the distinction between myelogenous leukemia and myelodysplasia is possibly arbitrary, as both conditions are part of a spectrum of disorders that are probably causally and mechanistically linked [5]. Atypical blood cells may or may not be present in the circulation, and it is likely that myelodysplasia, in cases that survive long enough, may progress to leukemia. We ruled out myelodysplasia, because the koala showed a rapid clinical outcome, only 19 days after initial onset (nasal hemorrhage) and a prominent leukocytosis ($295 \times 10^2/\mu l$; normal range, $3–10 \times 10^2/\mu l$) [12]. The limitation of our examination was a lack of bone marrow cytology and histopathology; however, regenerative hyperplasia of bone marrow cells including erythroblasts were possibly detected in blood smears in the present study. Nonregenerative anemia is one of the characteristics features of myelodysplastic syndromes [5]. We observed relatively higher number of erythroblasts (up to 30%) on blood smear from four koalas at age of 4 to 14 years without evidence of leukemia (Ito *et al*., unpublished data); therefore, koala might have a higher number of erythroblasts in peripheral blood even under physiological conditions. In the present case, acute leukemia could enhance regenerative extramedullary erythropoiesis observed in several organs including the spleen. Erythroleukemia was elucidated from a diagnosis, since atypia of erythroblasts was not identified in blood smears and tissue sections.

In this case, given that the tumor cells demonstrated presumable differentiation to atypical myeloid cells, and the acute onset of the disease, the most appropriate diagnosis is acute myelogenous leukemia.

ACKNOWLEDGMENT. The authors thank Mrs. Shigeko Suzuki for her technical assistance in preparing the histological specimens.

REFERENCES

1. Canfield, P. J. and Hemsley, S. 1996. Thymic lymphosarcoma of T cell lineage in a koala (Phascolarctos cinereus). *Aust. Vet. J.* **74**: 151–154. [Medline] [CrossRef]
2. Connolly, J. H., Canfield, P. J., Hemsley, S. and Spencer, A. J. 1998. Lymphoid neoplasia in the koala. *Aust. Vet. J.* **76**: 819–825. [Medline] [CrossRef]

3. Fiebig, U., Hartmann, M. G., Bannert, N., Kurth, R. and Denner, J. 2006. Transspecies transmission of the endogenous koala retrovirus. *J. Virol.* **80**: 5651–5654. [Medline] [CrossRef]
4. Hanger, J. J., Bromham, L. D., McKee, J. J., O'Brien, T. M. and Robinson, W. F. 2000. The nucleotide sequence of koala (Phascolarctos cinereus) retrovirus: a novel type C endogenous virus related to Gibbon ape leukemia virus. *J. Virol.* **74**: 4264–4272. [Medline] [CrossRef]
5. Hanger, J. J. and Loader, J. 2014. Disease in wild koalas with possible koala retrovirus involvement. *Technical Reports of the Australian Museum. Online (Bergh.)* **24**: 19–29.
6. Higgins, D. P. and Canfield, P. J. 2009. Histopathological examination of the pancreas of the Koala (Phascolarctos cinereus). *J. Comp. Pathol.* **140**: 217–224. [Medline] [CrossRef]
7. Kido, N., Edamura, K., Inoue, N., Shibuya, H., Sato, T., Kondo, M. and Shindo, I. 2012. Perivertebral B-cell lymphoma in a Queensland koala (Phascolarctos cinereus adustus) with paralytic symptoms in the hind limbs. *J. Vet. Med. Sci.* **74**: 1029–1032. [Medline] [CrossRef]
8. Miyazawa, T., Shojima, T., Yoshikawa, R. and Ohata, T. 2011. Isolation of koala retroviruses from koalas in Japan. *J. Vet. Med. Sci.* **73**: 65–70. [Medline] [CrossRef]
9. Oliveira, N. M., Farrell, K. B. and Eiden, M. V. 2006. In vitro characterization of a koala retrovirus. *J. Virol.* **80**: 3104–3107. [Medline] [CrossRef]
10. Shimizu, T., Yasuda, N., Kono, I. and Sakamoto, H. 1989. Diabetes mellitus in a koala (*Phascolarctos cinereus*). *Vet. Pathol.* **26**: 528–529. [Medline] [CrossRef]
11. Shojima, T., Yoshikawa, R., Hoshino, S., Shimode, S., Nakagawa, S., Ohata, T., Nakaoka, R. and Miyazawa, T. 2013. Identification of a novel subgroup of Koala retrovirus from Koalas in Japanese zoos. *J. Virol.* **87**: 9943–9948. [Medline] [CrossRef]
12. Tarlinton, R., Meers, J., Hanger, J. and Young, P. 2005. Real-time reverse transcriptase PCR for the endogenous koala retrovirus reveals an association between plasma viral load and neoplastic disease in koalas. *J. Gen. Virol.* **86**: 783–787. [Medline] [CrossRef]
13. Xu, W., Stadler, C. K., Gorman, K., Jensen, N., Kim, D., Zheng, H., Tang, S., Switzer, W. M., Pye, G. W. and Eiden, M. V. 2013. An exogenous retrovirus isolated from koalas with malignant neoplasias in a US zoo. *Proc. Natl. Acad. Sci. U.S.A.* **110**: 11547–11552. [Medline] [CrossRef]